Avalanches in a fluctuationless first-order phase transition in a random-bond Ising model

Eduard Vives and Antoni Planes
Departament d'Estructura i Constituents de la Matèria, Facultat de Física, Universitat de Barcelona, Diagonal 647, 08028 Barcelona, Catalonia, Spain
(Received 21 December 1993)

We study the behavior of the random-bond Ising model at zero temperature by numerical simulations for a variable amount of disorder. The model is an example of systems exhibiting a fluctuationless first-order phase transition similar to some field-induced phase transitions in ferromagnetic systems and the martensitic phase transition appearing in a number of metallic alloys. We focus on the study of the hysteresis cycles appearing when the external field is swept from positive to negative values. By using a finite-size scaling hypothesis, we analyze the disorder-induced phase transition between the phase exhibiting a discontinuity in the hysteresis cycle and the phase with the continuous hysteresis cycle. Critical exponents characterizing the transition are obtained. We also analyze the size and duration distributions of the magnetization jumps (avalanches).

I. INTRODUCTION

Among the wide variety of first-order phase transitions, there is a class for which thermal fluctuations are secondary. Prototypical examples are the solid-solid diffusionless martensitic transitions called athermal,[1] and some field-induced first-order transitions in ferromagnetic systems.[2] In the first case, when decreasing the temperature (T) the martensitic transition starts at a certain temperature but the system needs to be continuously cooled down to make the fraction (x) of the new phase increase. In the second case, the field (B) must be continuously changed in order to obtain a variation of the magnetization (m). In these two examples, in the two-phase coexistence range, the transition takes place instantaneously on macroscopic time scales, and then m (or x) do not depend on time (t) if B (or T) are kept constant. The two external parameters T and B play a similar role: they determine the free-energy difference between the two phases, which provides the driving force for the transition.

Hysteresis in the (B,m) or (T,x) plane is inherent to all such processes. It is worth noting that this hysteresis is persisting even though the changes of B or T are carried out exceedingly slow, showing that this hysteresis is not of kinetic nature but associated to the existence of intrinsic disorder in the system.[3] Usually the hysteresis cycles show the interesting return-point-memory (RPM) property:[4] when driving the system by changing the external field $[B(t)]$, the magnetization $[m(t)]$ depends on the previous history only through the memory of the points where $B(t)$ has been reversed. It is necessary, but by no means enough, that thermal fluctuations do not play a role for this RPM property to be satisfied.[5,6]

Accurate observations reveal that, for this kind of processes, when changing the external field, the transition proceeds through fast avalanches. These avalanches connect metastable states separated by very-high-energy barriers ($\gg kT$). They have been experimentally studied in the case of martensitic transitions[7] and in the case of field-induced change of magnetization in ferromagnetic systems (Barkhausen effect).[8] The striking result is that size and lifetime distributions of such avalanches follow power laws. It has been suggested, in both cases, that the theory of self-organized criticality (SOC) applies to such systems. This theory, recently introduced by Bak, Tang, and Wiesenfeld,[9] proposes that externally driven systems with spatial and temporal degrees of freedom, evolve until a critical state is reached, in which the avalanches show no characteristic temporal and spatial scales. In the case of magnetic systems, the abrupt and stochastic response of the magnetization to an external field arises from the intricate character of interactions, internal stresses and defects in the system. A similar situation occurs during the growth of the low-temperature phase in systems undergoing martensitic transitions. A detailed study of this behavior appears to be very complicated. A simple way of considering the effect of the competing interactions and defects is to introduce some kind of random disorder on simple models. With this idea in mind, Sethna *et al.*[5] have recently considered a random-field Ising model (RFIM) at zero temperature to study the hysteretic behavior in athermal first-order phase transitions. Changing the external field, the obtained hysteresis loops show the RPM property. Moreover, changing the amount of disorder they detect a phase transition from a situation in which the hysteresis cycle shows an "infinite" (or percolating) avalanche to a situation where all avalanches are "small." The transition takes place at a critical value of disorder for which the avalanches have no characteristic length scale.

In this paper we consider a different model: the random-bond Ising model (RBIM) (or Edwards-Anderson spin-glass model).[10] The disorder is not introduced as a static random field but on the spin-spin interactions, mimicking the complex (magnetic or elastic) interactions between the transformed and nontransformed domains. We study the evolution of the system at zero temperature when the external field is changed. Contrarily to the RFIM case, the return-

point-memory property is not satisfied. As in the RFIM, the model also shows a disorder-induced phase transition. We concentrate in the study of such phase transition between the situation with infinite avalanche to the finite avalanche behavior. The universal characteristics of this transition are studied by finite-size scaling analysis. The size distribution of avalanches is also studied as a function of the degree of disorder in the system. The results are finally discussed in the context of the SOC theory, the percolation theory, and recent experimental results in magnetic and martensitic systems.

II. MODEL

We consider the standard RBIM model[10] for a spin glass. The system is defined on a two-dimensional $L \times L$ square lattice. On each site we define a spin variable s_i ($i=1,\ldots,N=L^2$) taking values ± 1. The Hamiltonian is

$$H=\sum_{i,j} J_{ij}s_i s_j - B\sum_{i=1}^{N} s_i \ , \tag{1}$$

where J_{ij} are the coupling constants, B is an homogeneous external field and the first summation extends over all the nearest-neighbors pairs. The J_{ij} are chosen randomly according to a Gaussian distribution with fixed mean value $\bar{J}=\sum_{ij} J_{ij}/2N=-1$ and standard deviation σ, i.e.:

$$P(J)=(2\pi\sigma^2)^{-1/2}e^{-(J+1)^2/2\sigma^2} \ . \tag{2}$$

Such models with intrinsic quenched disorder show interesting fundamental problems. Most of the studies in the literature correspond to the RBIM model with infinite range interaction, also known as the Sherrington-Kirpatrick model.[11,12] For this, the mean-field solution ought to be exact, and the results are, in fact, independent of the exact distribution of J_{ij} (they depend only on $\bar{J}$ and σ). The presumed exact phase diagram for the Sherrington-Kirpatrick model with zero external field shows a phase transition at $T=0$ from a spin-glass ferromagnetic phase for $\sigma/\bar{J}<1$ to a pure spin-glass phase for higher $\sigma/\bar{J}$. Much less is known for short-range models. For this case, most of the studies correspond to symmetrical models with $\bar{J}=0$. The only nonsymmetrical model, which has been studied is the $\pm J$ model, which has random bonds with values ± 1.[13] On a square lattice, when the concentration p of antiferromagnetic bonds exceeds a critical value p_c one expects a transition from a ferromagnetic phase to a spin-glass phase (although there is some discussion on the nature of this spin-glass phase).[14] The critical value p_c is associated to the percolation of nonfrustrated "plaquettes."[15] Estimations based on different approaches give values around $p_c \sim 15\%$.[11,16]

To study the evolution of the system defined by (1) when the external field B is changed, dynamic rules must be specified. We have chosen deterministic rules corresponding to an energy relaxation process. For very high fields $B \gg 0$ the ground state has all the spins $s_i=1$. When decreasing the field the system relaxes by flipping spins, until the state with all the spins down $s_i=-1$ is reached when $B \ll 0$. The energy change associated to an individual spin-flip is

$$\Delta H_i=-2s_i\{B_i-B\} \ , \tag{3}$$

where B_i is the internal field acting on spin s_i

$$B_i=\sum_j J_{ij}s_j \ . \tag{4}$$

The spin s_{i0} with highest internal field B_{i0} will become unstable and will flip when B reaches the value B_{i0} from above. After this flip the internal fields on the neighboring spins are updated. Then it may happen that some of them become unstable and an avalanche starts. Two different mechanisms can be adopted. (a) Synchronous dynamics: all the unstable spins are flipped simultaneously and, afterwards, all the B_i are updated again. (b) Sequential dynamics: the most unstable spin is flipped first and the neighboring B_i are updated afterwards.

In both cases the algorithm is repeated until an equilibrium situation is reached, i.e., all the spins with $B_i > B$ are negative and all the spins with $B_i < B$ are positive. This is the end of the avalanche. The external field may then be decreased until a new spin becomes unstable. In the present work we have chosen the first mechanism, which is more similar to the simultaneous updating algorithms used for the study of cellular automata.[17] One of the advantages of the simultaneous dynamics is that it enables to distinguish between the avalanche size (number of spins flipped during the avalanche) and the avalanche duration (number of times that the algorithm is repeated until equilibrium is reached), which gives information on the propagation "speed" of the avalanche. Nevertheless, we have compared both dynamics (sequential and parallel) and obtained that they give qualitatively the same results in connection to the avalanche sizes.

We have performed computer simulations at zero temperature on finite systems with sizes ranging between $L=10$ and 100. The interaction bonds J_{ij} are initially generated with a standard Gaussian random number generator. For each size, ensemble averages over a large number of equivalent systems (up to 5000), generated with different seeds for the random number generator, have been taken.

III. HYSTERESIS CYCLES

Figure 1 shows three typical hysteresis cycles of the total magnetization $M=\sum_{i=1}^{N} S_i$ corresponding to a $L=40$ system for different values of the amount of disorder σ. For low disorder values the cycle shows big jumps (avalanches), while for high disorder values the cycle is smoother and extends up to higher B values. For the nondisordered system with all $J_{ij}=-1$ the cycle would be perfectly rectangular with avalanches at $B=\pm 4$ flipping all the spins. For any small amount of disorder the behavior is rather different. The first small avalanche starts at the spin with smallest B_i (which depends very much on the particular realization of the random number generator). For a field value close to $B \sim -2$ an avalanche with size proportional to L^2 (we will call it

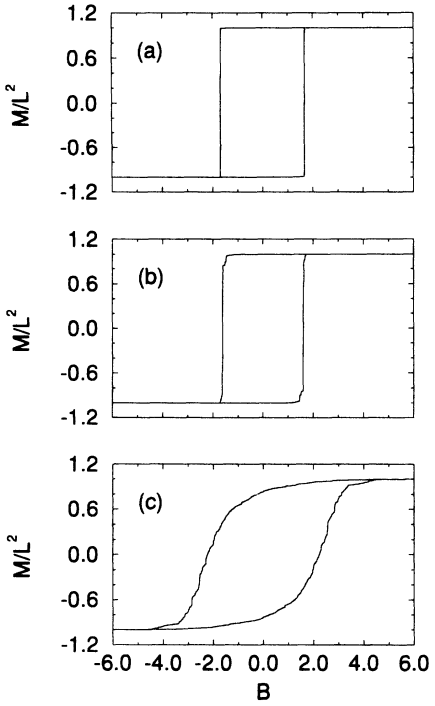

FIG. 1. Examples of hysteresis cycles for a system of size $L=40$ and $\sigma=0.45$ (a), 0.55 (b), and 1.5 (c).

infinite avalanche) starts and lasts for a number of steps proportional to L.

The hysteresis cycles are always symmetric, since the Hamiltonian is invariant under changes $+s_i \rightarrow -s_i$ and $B \rightarrow -B$. We have also studied the behavior of the system when the external field evolution is reversed at a stable point with $M/L^2 \neq \pm 1$ (partial cycling). Figure 2 shows an example of a partial cycle, evidencing that the RPM property is not satisfied in our model. This is due to the fact that reverse spin flip may occur during an avalanche, since antiferromagnetic bonds are present on the system. This destroys the dynamical partial ordering of the metastable states necessary for the RPM property to be fulfilled[6,5] although, for the values studied ($\sigma < 2$) the amount of such reverse flips is a very small fraction compared to the total number of flips. Such reversal spin-flips can never happen in the RFIM at zero temperature in which the RPM property is satisfied.[5] Scanning electron microscopy of real systems undergoing martensitic transitions (e.g., Cu-Zn-Al) has revealed sometimes the reversal of transformed domains,[18] providing a justification for the use of the RBIM rather than the RFIM for the modeling of such systems.[19]

It is interesting to note that a first look to the cycles of Fig. 1 and the similar ones corresponding to other system sizes already suggests the existence of a transition between a phase with low disorder exhibiting an infinite avalanche when cycled and a phase with high disorder exhibiting no such infinite avalanche.

IV. CRITICAL BEHAVIOR

In order to study such a disorder induced transition, for each full hysteresis cycle, we have measured the size m_0 of the biggest avalanche and the duration t_0 of the longest avalanche for systems of different sizes and for different values of the parameter σ. Figures 3 and 4 show the behavior of the average values of m_0 and t_0, respectively. The error bars correspond to the measure of the statistical deviations. The sharp change in $\langle m_0 \rangle$ and the pronounced peak in $\langle t_0 \rangle$ reveal the existence of such a transition between a behavior with infinite avalanche and a behavior with only small avalanches.

The behavior of the curves $\langle m_0 \rangle$ and $\langle t_0 \rangle$ as a function of the amount of disorder σ for different system sizes (L) resembles the behavior of the long-range order parameter and relaxation time in a second-order phase transition. We then assume that standard scaling arguments are suitable in order to study the transition. Such an assumption will be supported afterwards by the good agreement found with the simulation data.

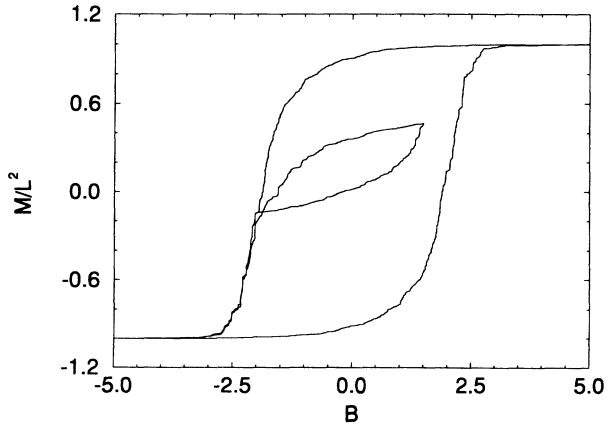

FIG. 2. Full hysteresis cycle and partial cycle for a system of size $L=40$ and $\sigma=1.2$. After the partial cycle, the different evolution reveals that the return point memory effect does not hold in our system.

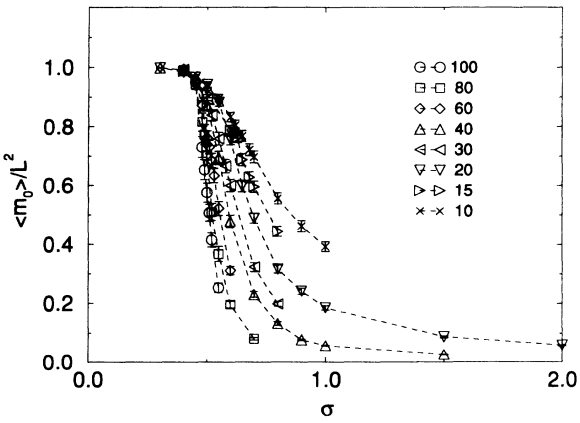

FIG. 3. Behavior of the mean size $\langle m_0 \rangle$ of the largest avalanche for different values of the amount of disorder σ and different system sizes indicated on the legend. Error bars correspond to the standard deviations from the mean values. Dashed lines are guides to the eye.

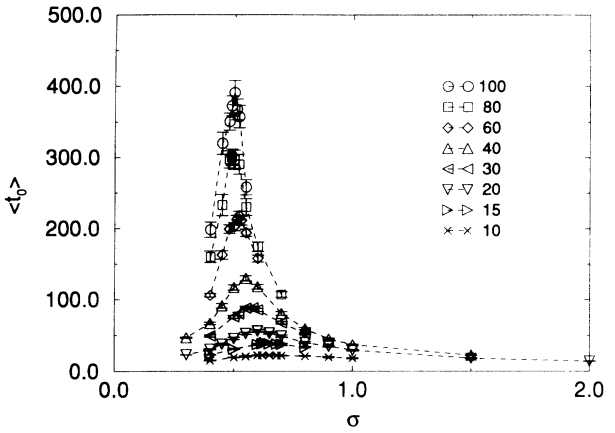

FIG. 4. Behavior of the mean duration $\langle t_0 \rangle$ of the largest avalanche for different values of the amount of disorder σ and different system sizes indicated on the legend. Error bars correspond to the standard deviations from the mean values. Dashed lines are guides to the eye.

A. Scaling hypotheses

We suppose the existence of a correlation length in the system ξ, which for the infinite system diverges at a critical value σ_c as

$$\xi \sim \left| \frac{\sigma - \sigma_c}{\sigma_c} \right|^{-\nu} . \tag{5}$$

The scaling hypothesis consists in assuming that any other quantity A exhibiting a nonanalytical behavior at σ_c will behave as

$$A \sim \xi^{\alpha} \sim \left| \frac{\sigma - \sigma_c}{\sigma_c} \right|^{-\nu\alpha} . \tag{6}$$

In particular, the mean duration of the largest avalanche diverges with an exponent z as

$$\langle t_0 \rangle \sim \xi^{z} \sim \left| \frac{\sigma - \sigma_c}{\sigma_c} \right|^{-\nu z} . \tag{7}$$

For a finite system with size L standard finite-size scaling corrections should be applied. The transition will take place at a pseudocritical disorder $\sigma_c(L)$ at which the correlation length equals a fraction of the size of the system, $\xi = KL$. This pseudocritical temperature can be estimated from the position of the inflections or peaks in the different variables which, for the infinite system, will show a nonanalytical behavior. From Eq. (5) one immediately gets

$$\sigma_c(L) = \sigma_c + S_0 L^{-1/\nu} , \tag{8}$$

where S_0 is a constant, which depends on the particular way used for the estimation of $\sigma_c(L)$. As $\sigma \to \sigma_c(L)$, the correlation length for the finite system behaves as

$$\xi = L |\tilde{\sigma}_L L^{1/\nu} + X_0|^{-\nu} , \tag{9}$$

where X_0 is a constant, and $\tilde{\sigma}_L$ is the reduced disorder for the finite system:

$$\tilde{\sigma}_L = \frac{\sigma - \sigma_c(L)}{\sigma_c(L)} . \tag{10}$$

Substituting (9) in (6) one gets the general behavior of any quantity A close to the pseudocritical temperature for a finite system:

$$A \sim L^{\alpha} F_A(L^{1/\nu} \tilde{\sigma}_L) , \tag{11}$$

where F_A is the scaling function and $L^{1/\nu}\tilde{\sigma}_L$ is the scaling variable.

B. Scaling results for $\langle t_0 \rangle$ and $\langle m_0 \rangle$

According to Eq. (11), $\langle t_0 \rangle$ should behave with system size as

$$\langle t_0 \rangle \sim L^{z} F_{\langle t_0 \rangle}(L^{1/\nu} \tilde{\sigma}_L) \tag{12}$$

and the behavior of the peak height and the peak curvature (in Fig. 4) will be given by

$$\langle t_0 \rangle_{\sigma = \sigma_c(L)} \sim L^{z} , \tag{13}$$

$$\left. \frac{d^2 \langle t_0 \rangle}{d\sigma^2} \right|_{\sigma = \sigma_c(L)} \sim L^{z+2/\nu} . \tag{14}$$

Using parabolic fits to estimate the peak position, peak height and curvature one can calculate z and ν. Figures 5 and 6 show in log-log plots the behavior of $\langle t_0 \rangle_{\sigma = \sigma_c(L)}$ and $(d^2\langle t_0 \rangle / d\sigma^2)|_{\sigma = \sigma_c(L)}$ as a function of L, respectively. Linear fits give $z = 1.2 \pm 0.1$ and $\nu = 1.4 \pm 0.1$. With such estimations for the critical exponents we can test the scaling assumption (12) by plotting $\langle t_0 \rangle / L^{z}$ as a function of the scaling variable. The resulting scaling function $F_{\langle t_0 \rangle}$ is displayed in Fig. 7 and shows a very good overlap of the different curves corresponding to the different system sizes.

A similar treatment can be done with $\langle m_0 \rangle$. According to Eq. (11), the finite-size scaling behavior for its singular part is

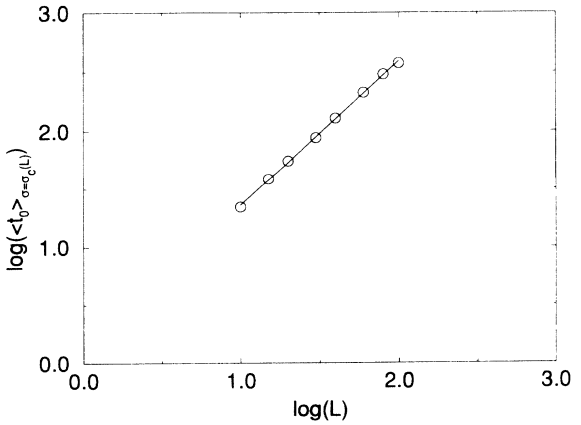

FIG. 5. Log-log plot of the peak position of the functions $\langle t_0 \rangle(\sigma)$ as a function of L. The line is a least-squares fit.

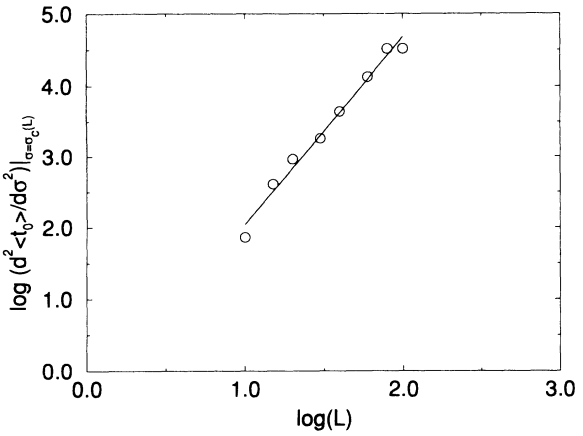

FIG. 6. Log-log plot of the curvature at the peak position of the functions $\langle t_0 \rangle$ as a function of L. The line is a least-squares fit.

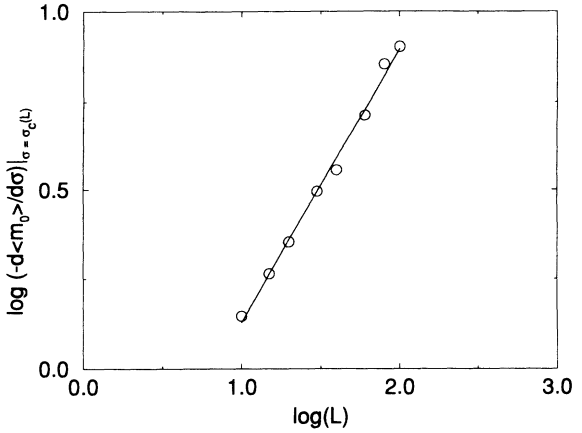

FIG. 8. Log-log plot of the slope at the inflection point of the functions $\langle m_0 \rangle$ as a function of L. The line is a least-squares fit.

$$\langle m_0 \rangle / L^2 \sim L^{\beta} F_{\langle m_0 \rangle}(L^{1/\nu} \tilde{\sigma}_L) . \quad (15)$$

By polynomial fits we obtain estimations of the position of the inflexion point, the value of $\langle m_0 \rangle / L^2$ and the first derivative at that inflection point. The statistical errors of the data do not allow to obtain a good estimation of the β exponent. From the log-log plots of the first derivatives (shown in Fig. 8) one gets $\beta = 0.065 \pm 0.1$. Such result ($\beta \simeq 0$) is also consistent with the fact that $\langle m_0 \rangle / L^2$ has a constant value (independent of L) at the pseudocritical point ($\langle m_0 \rangle / L^2 = 0.604 \pm 0.01$). Figure 9 shows the scaling of the different $\langle m_0 \rangle / L^2$ curves according to Eq. (15).

From the estimations of $\sigma_c(L)$ obtained from the positions of the peak height of $\langle t_0 \rangle$ and the inflection points of $\langle m_0 \rangle / L^2$ it is possible to verify Eq. (8). Figure 10 shows the behavior of $\sigma_c(L)$ versus $L^{-1/\nu}$ ($\nu = 1.4$) displaying the expected linear behavior for $L \geq 20$. Least-squares fits give, in the limit $L \to \infty$, $\sigma_c = 0.436$ and 0.446, respectively, from the two different estimations. These two values, together with a third way of measuring $\sigma_c(L)$, which will be presented in Sec. V, give data compatible with a critical value $\sigma_c = 0.44 \pm 0.01$.

Besides the mean value of m_0, we have also measured the full distribution $p(m_0)$ by doing statistics over a very large number of equivalent runs. Figure 11 shows the distributions corresponding to a system of size $L = 40$ at $\sigma = 0.5 < \sigma_c(L)$, $\sigma = 0.58 \simeq \sigma_c(L)$, and $\sigma = 0.75 > \sigma_c(L)$. The behavior corresponds to the one found in a second-order phase transition with a very broad and flat distribution at the phase transition, and no coexisting peaks.

V. AVALANCHE DISTRIBUTIONS

In the preceding section we have studied the behavior of the biggest avalanche m_0. Now we concentrate in the study of the size and duration distribution of all the avalanches appearing in the hysteresis cycle.

Figure 12 shows examples of the full avalanche size distribution $p_{\sigma,L}(m)$, in log-log scales, for a system with

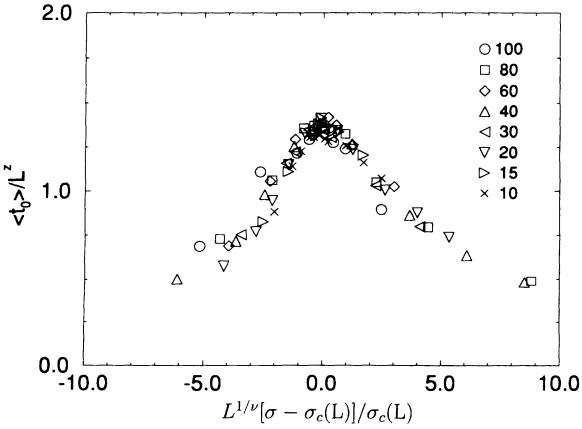

FIG. 7. Scaling of the functions $\langle t_0 \rangle$ from Fig. 4. The legend indicates the different system sizes.

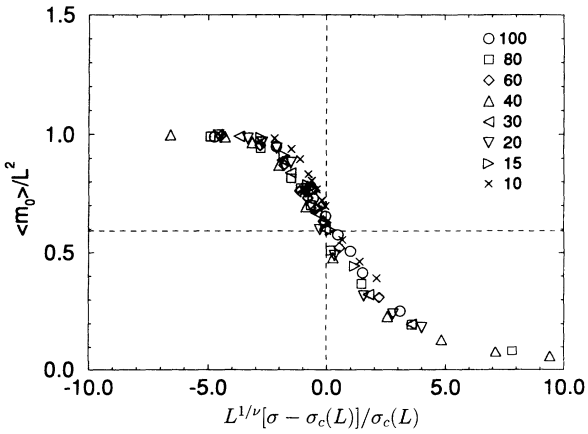

FIG. 9. Scaling of the functions $\langle m_0 \rangle$ from Fig. 3. The legend indicates the different system sizes. The horizontal dashed line indicates the value $m_0/L^2 = 0.5928$, which is the size of the percolating cluster.

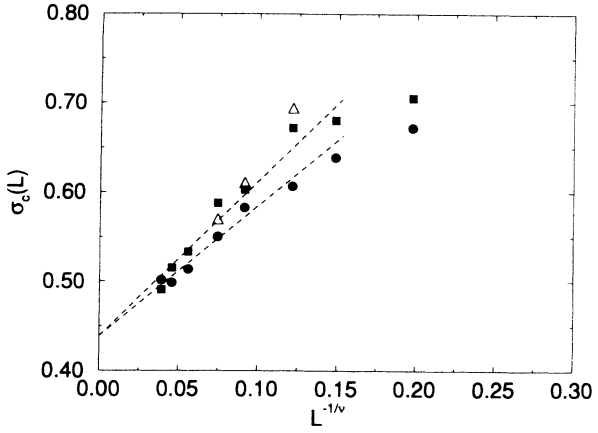

FIG. 10. Linear behavior of $\sigma_c(L)$ in front of $L^{-1/\nu}$. Full circles correspond to the estimations from the peak in $\langle t_0 \rangle$, full squares to the inflection point in $\langle m_0 \rangle$, and the open triangles to the values for which the exponential contribution to the avalanche size distribution vanishes, giving a pure power-law behavior. The lines are guides to the eye, indicating the compatibility with a linear behavior with a common limiting value.

$L=40$ at three different values of σ, below, approximately at, and above the critical value $\sigma_c(L) \sim 0.55$. The distributions have been normalized by the total number of avalanches. The statistical errors increase enormously with decreasing σ because of the decrease of the total number of avalanches. The histogram at $\sigma=1.5$ has been obtained after averaging over ~ 100 runs, while the histograms at $\sigma=0.55$ and 0.45 correspond to averages over ~ 5000 runs. A first sight reveals that for $\sigma > \sigma_c(L)$ the distribution decays faster than a power law (subcritical behavior), at $\sigma \sim \sigma_c(L)$ the behavior is compatible with a power law (critical behavior), and for $\sigma < \sigma_c(L)$ a peak appears at high values of m, corresponding to the infinite avalanche distribution [$p(m_0)$, see Fig. 11] and the distribution at low m values seems to decay slower

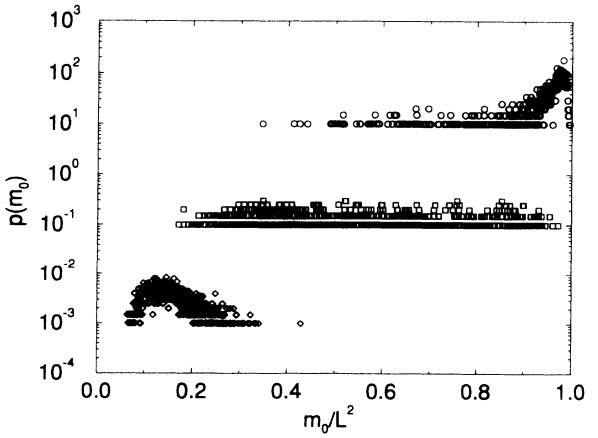

FIG. 11. Semilogarithmic plot of the distribution of the biggest avalanche $p(m_0)$ for a system with $L=40$ and at $\sigma=0.5<\sigma_c(L)$ (circles), $\sigma=0.58\sim\sigma_c(L)$ (squares), and $\sigma=0.75>\sigma_c(L)$ (diamonds). The two upper curves are shifted two and four decades, respectively.

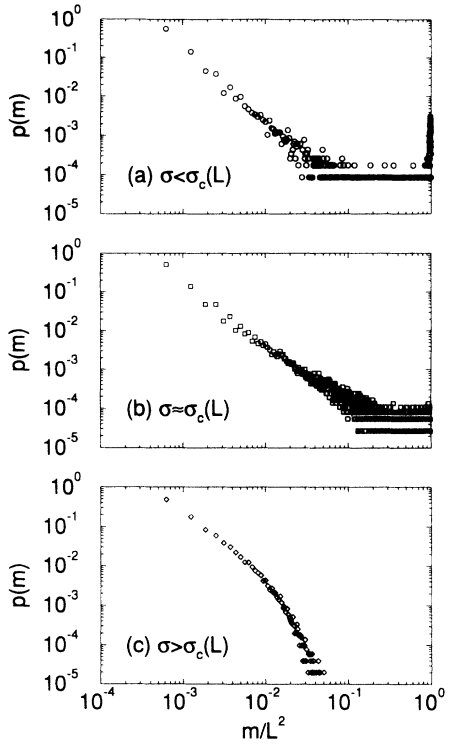

FIG. 12. Log-log plots of the avalanche size distributions for a system with $L=40$ at $\sigma=0.45<\sigma_c(L)$ (circles), $\sigma=0.55\sim\sigma_c(L)$ (squares), and $\sigma=1.5>\sigma_c(L)$ (diamonds).

than a power law (supercritical behavior).

To analyze such behavior we extend the above finite-size scaling considerations, assuming for $p_\sigma(m)$:

$$p_\sigma(m) \sim e^{-K(m/\xi^2)^x} m^{-\tau}, \tag{16}$$

where K is a constant that changes its sign at the transition point. Such a function reproduces the behavior of Fig. 12, except for the presence of the peak at great values of m/L^2 when $\sigma < \sigma_c$. We will restrict ourselves to the study of the distributions at low values of m/L^2. At the critical point $\xi \to \infty$, the distribution (16) is a power law, while out of criticality we have a positive or negative exponential prefactor. The dependence of the exponential factor with m/ξ^2 comes from the fact that we found $\beta \sim 0$ in Eq. (15). Perhaps a dependence with $m/\xi^{2+\beta}$ would be more suitable, but our statistical errors do not enable a reliable fit to such a behavior. Using Eq. (5) one gets for the infinite system:

$$p_\sigma(m) \sim m^{-\tau} e^{-K[m(\sigma-\sigma_c/\sigma_c)^{2\nu}]^x}. \tag{17}$$

This phenomenological assumption is similar to the one known as "Fisher droplet" for the cluster distribution in the percolation problem.[20] It reduces to it when $x=1/2\nu$.

By using Eq. (9) one can deduce the scaling assumption for the finite system:

$$p_{\sigma,L}(m) \sim m^{-\tau} e^{-f(\bar{\sigma}L^{1/\nu})(m/L^2)^x}, \tag{18}$$

which is of the same kind as proposed by Kadanoff[21] for two-dimensional cellular automata. This expression can

be easily fitted by taking its logarithmic derivative:

$$\frac{d\ln[p(m)]}{d\ln(m)} = -\tau - xf(\tilde{\sigma}L^{1/\nu})(m/L^2)^x . \quad (19)$$

From the simulated data one can numerically compute the logarithmic derivative using

$$\frac{d\ln[p(m)]}{d\ln(m)} \sim \frac{\ln[p(\alpha m)/p(m)]}{\ln(\alpha)} , \quad (20)$$

where α is a parameter, which has to be chosen as small as possible. Taking $\alpha=5$ we have computed the derivatives of all the distributions for systems of size $L=20$, 30, and 40 and different values of σ below and above the transition points. Figure 13 shows, as an example the behavior of the logarithmic derivatives for $L=30$ and $\sigma=0.55$, 0.60, and 0.65. Although the numerical errors are important, the behavior can be considered to be linear up to $m/L^2=0.2$, indicating that the value $x=1$ is a good approximation, at least for low values of m/L^2. The value of the derivative at $m\to 0$ gives an estimation of the exponent τ. Within the scatter of the data it is the same above and below the transition, confirming the consistency of our finite-size-scaling assumption. The slope $f(\tilde{\sigma}L^{1/\nu})$ changes sign above and below the transition. In fact, $f(\tilde{\sigma}L^{1/\nu})=0$ gives a new estimation of $\sigma_c(L)$, which we have already plotted in Fig. 10 using open triangles.

In Fig. 14 we have plotted the fitted values of τ versus $\tilde{\sigma}L^{1/\nu}$ for the three different system sizes, using $\sigma_c(L)$ estimations as explained in the previous paragraph. The plot shows that all the data are consistent with a constant value of $\tau=1.45\pm0.1$ inside the critical region, which extends, at least, from $\tilde{\sigma}=-1.5$ to $\tilde{\sigma}>5.0$. The change in the τ exponent for low values of disorder could be associated to the end of the critical region or to the statistical errors in that zone where the number of avalanches is very small and the resolution of the histograms is poorer. Figure 15 shows the behavior of the function $f(\tilde{\sigma}L^{1/\nu})$, which also shows a good scaling behavior for the different system sizes. Note that its behavior is quite linear, which means that the avalanche size distribution, for small values of m, is in fact

$$p_{\sigma,L}(m) \sim m^{-\tau} e^{-C(\tilde{\sigma}L^{1/\nu})(m/L^2)} . \quad (21)$$

We have also considered the distribution of durations of the avalanches $p_{\sigma,L}(t)$. A detailed finite size scaling analysis has not been performed in this case, although the same methodology used for $p_{\sigma,L}(m)$ can be applied. Figure 16 summarizes three examples of unnormalized dis-

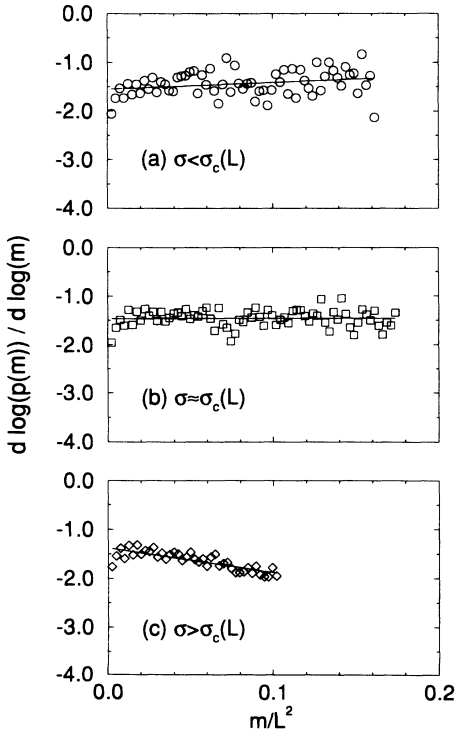

FIG. 13. Logarithmic derivatives of the avalanche size distributions for a system of size $L=30$ at $\sigma=0.55<\sigma_c(L)$ (circles), $\sigma=0.60\sim\sigma_c(L)$ (squares), and $\sigma=0.75>\sigma_c(L)$ (diamonds). The lines are least-squares fits.

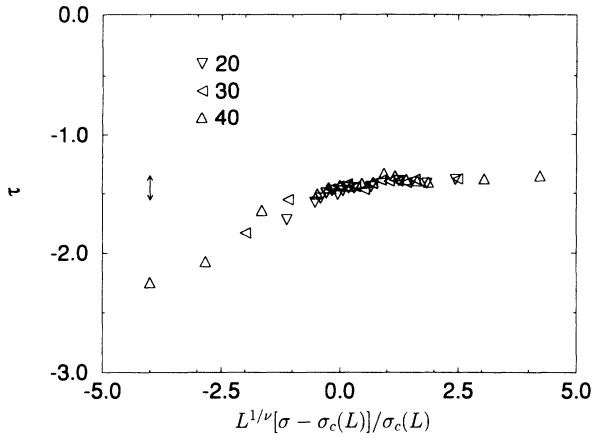

FIG. 14. Fitted values of the τ exponent for different system sizes (see legend) and different temperatures in front of the scaling variable. For a broad region, the value of τ is almost constant around the value -1.45 ± 0.1 indicated by the arrowed line.

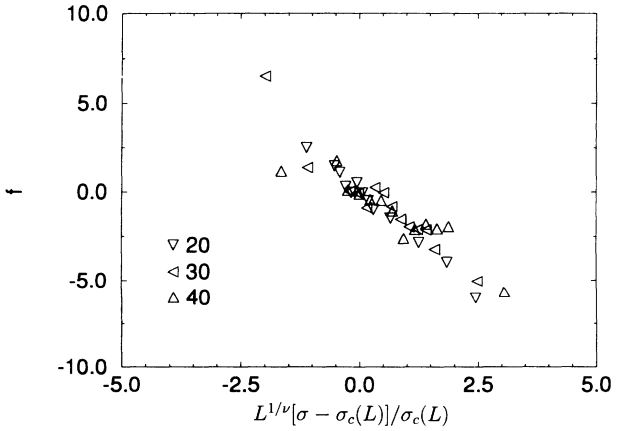

FIG. 15. Behavior of the function f in front of the scaling variable for different system sizes as indicated in the legend.

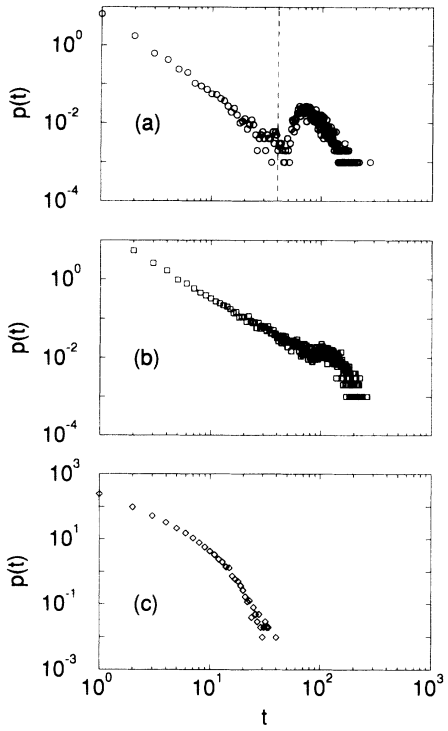

FIG. 16. Log-log plots of the avalanche duration distributions for a system with $L=40$ at $\sigma=0.45<\sigma_c(L)$ (circles), $\sigma=0.55\sim\sigma_c(L)$ (squares), and $\sigma=1.5>\sigma_c(L)$ (diamonds). The dashed line on the upper figure indicates the $t=L$ value.

tributions, corresponding to a system with $L=40$ and (a) $\sigma=0.45<\sigma_c(L)$, (b) $\sigma=0.55\sim\sigma_c(L)$ and (c) $\sigma=1.5>\sigma_c(L)$. The distributions are averaged over ~ 5000, ~ 5000, and ~ 100 different runs, respectively. The behavior for both $\sigma>\sigma_c$ and $\sigma<\sigma_c$ seem to be exponentially damped, while at criticality a power law can be fitted over two decades, rendering an exponent for the critical time distribution $\mu=1.65\pm0.1$. The exponential factor above and below the transition can be handled by using an expression similar to Eq. (16) but with a constant K not changing sign at the transition. The peak appearing for $\sigma<\sigma_c(L)$ corresponds to the duration of the percolating avalanche, which is always longer than L steps (in this case $L=40$). This peak shifts to that value $L=40$ as σ decreases.

VI. DISCUSSION

From the above finite-size analysis of the RBIM model we have characterized the disorder-induced phase transition appearing at $\sigma_c=0.44\pm0.01$ by the set of critical exponents presented in Table I. We expect these exponents to be independent of many details of the system but to depend on dimensionality, symmetries, etc.

Some of the results suggest a close relation between the observed phase transition and the bond percolation phenomenon:[20] briefly, this geometrical phenomenon appears on, for instance, a two-dimensional (2D) square lattice when a fraction x of the bonds is removed. If the fraction is less than a critical value $x_c=0.5$ one can still identify a cluster of connected sites, which extends over all the system (percolating cluster). If $x>x_c$, it is not possible to find such a percolating cluster. There are two interesting points linking the phase transition in the RBIM with the percolation problem. First, the number of sites of the percolating cluster at $x=x_c$ is known to be 0.5928 (indicated by the vertical dashed line in Fig. 9), very close to the size of the critical avalanche in the RBIM, $\langle m_0\rangle/L^2=0.604\pm0.01$. This means that the phase transition occurs for the value of σ at which the biggest avalanche percolates. Second, the value of the exponent ν for the percolation problem is $\nu=4/3$ also very close to the value we have found (see Table I). It is difficult to further extend the comparison: in particular, it is not evident to establish a relation between the fraction of antiferromagnetic bonds in our problem ($\sigma_c=0.44$ corresponds to a 1.16% of antiferromagnetic bonds) and the fraction of broken bonds in the percolation problem.

The obtained results concerning the avalanche size and duration distributions also suggest a relation with the SOC theory. This concept applies to such externally driven systems that spontaneously organize, without fine tuning of any parameter, in a persisting marginally stable state with propagating avalanches of all sizes. In our model the SOC idea cannot strictly be applied, since the critical state only stands for a finite range of the external field driving the transition, as discussed in Ref. 24. In addition to this criticism, we need the fine tuning of the amount of disorder σ in order to reach such a critical state. Despite that, for real systems (magnetic and martensitic), the SOC theory, has been used, in a less strict way, to explain the apparition of avalanches showing power-law distributions. In these systems, the critical

TABLE I. Fitted critical exponents for the RBIM disorder-induced phase transition.

Quantity	Definition	Value
Correlation length	$\xi\sim\left[\frac{\sigma-\sigma_c}{\sigma_c}\right]^{-\nu}$	$\nu=1.4\pm0.1$
Mean duration of the largest avalanche	$\langle t_0\rangle\sim\xi^{-z}$	$z=1.2\pm0.1$
Mean size of the biggest avalanche	$\langle m_0\rangle\sim\xi^{-\beta}$	$\beta=0.065\pm0.1$
Avalanche size distribution at $\sigma=\sigma_c$	$p(m)\sim m^{-\tau}$	$\tau=1.45\pm0.1$
Avalanche duration distribution at $\sigma=\sigma_c$	$p(t)\sim t^{-\mu}$	$\mu=1.65\pm0.1$

state also appears only for a finite range of the driving field (or temperature), so the same former criticism stands. We propose that for such experimental systems exhibiting fluctuationless first-order transitions, our model or similar ones, would be more suitable than the SOC theory, in order to explain the apparition of the power-law distributions. For such an explanation, the important question to be answered is why the experimental systems appear to self-stay at the critical amount of disorder. We guess two possible answers to that question. (i) The experimental errors make difficult to distinguish the existence of an exponential prefactor, especially if the distributions are measured in a too limited range of avalanche sizes (as usually happens). Careful reanalysis of data has, in the problem of rearrangement of magnetic domains,[22] revealed the existence of a subcritical behavior.[23] (ii) A more subtle explanation would be that internal relaxations spontaneously modify the amount of disorder present in the system until the critical disorder is reached. There are experimental basis for this idea in the particular case of systems undergoing martensitic transitions. It has been observed that the hysteresis cycles are strongly dependent upon the heat treatment (which controls the quenched-in disorder) of the sample. For samples slowly cooled from high temperature, the defect concentration is very low and the cycle displays very large avalanches [such as the cycle shown in Fig. 1(a)], while for samples directly quenched (higher concentration of defects) the cycle displays only tiny avalanches [such as Fig. 1(c)]. Moreover, it is also known that after a number of cycles, the hysteresis loop evolves towards a behavior quite independent of the initial heat treatment. In fact, the experimental measurements showing power-law distributions of avalanche size and duration have been carried out precisely after a large number of cycles, when presumably the final critical attractor has been reached.

Finally, in relation with the power-law behavior of the distributions at the critical point ($\sigma=\sigma_c$), it should be mentioned that the values of τ and ν have also been measured in the RFIM (Ref. 5) giving $\tau=2.0\pm0.03$ and $\nu=1.0\pm0.1$. The comparison is questionable, since these values correspond to a 3D case, while our case is two dimensional. In the context of assumption (ii) in the above paragraph, we can also try to compare with experimental data corresponding to systems, which will supposedly be at criticality. The avalanche size distribution and its exponent τ is experimentally difficult to measure, but there are measurements available for the exponent μ of the distribution of durations, which might be independent of the dimensionality. For the martensitic transition in Cu-Zn-Al,[7] it has been found that $\mu=1.6\pm0.3$, and for the rearrangement of magnetic domains,[22] $\mu\simeq1.59$ is in good agreement with the present results.

VII. SUMMARY AND CONCLUSIONS

In this paper we have considered a 2D RBIM (spin-glass model) at zero temperature as a simple model for the study of those first-order phase transitions on solids for which thermal fluctuations are secondary (we call them fluctuationless first-order phase transitions). The spin-spin interaction constants obey a Gaussian distribution with fixed mean value and standard deviation σ. The value of σ is a measure of the amount of disorder in the system. At zero temperature, when sweeping the external field from high positive values to high negative values, the system undergoes a first-order phase transition. When disorder is present ($\sigma\neq0$), the transition does not take place at a single value of the field but in a range of values and shows intrinsic hysteresis, depending on the amount of disorder in the system. This is qualitatively similar to what is observed in systems like ferromagnetic materials and metallic alloys undergoing martensitic transitions. Even if thermal fluctuations are absent in our system, reverse spin flip can occur during the evolution, which destroys the necessary partial ordering of metastable states[6] for the return-point-memory property to be fulfilled.

When the amount of disorder σ is changed the system exhibits a phase transition between an hysteretic behavior with a percolating avalanche ($\sigma<\sigma_c$) to a situation without percolating avalanches ($\sigma>\sigma_c$). By using finite-size scaling we have studied the critical behavior of the system close to the critical point ($\sigma_c=0.44$). The quantities exhibiting nonanalytical behavior when $\sigma\rightarrow\sigma_c$ have been characterized by a number of critical exponents summarized in Table I.

Concerning the avalanches, our results show that the size distributions exhibit a power-law behavior with an exponential prefactor, which becomes a constant at criticality ($\sigma=\sigma_c$). Away from criticality the system shows subcritical (when $\sigma>\sigma_c$) or supercritical (when $\sigma<\sigma_c$) behavior depending on the sign of the exponent of the prefactor. A similar behavior is observed for the duration distribution of the avalanches. The model provides a useful basis for the description of experimental systems exhibiting fluctuationless first-order phase transitions.

ACKNOWLEDGMENTS

We acknowledge Lluís Mañosa, Jordi Ortín, and Jürgen Goicoechea for fruitful comments and the Comisión Interministerial de Ciencia y Tecnología (Spain) for financial support under Project No. MAT92-884.

[1]W. Cao, J. A. Krumhansl, and R. J. Gooding, Phys. Rev. B **41**, 11 319 (1990).

[2]D. A. Everett and W. I. Whitton, Trans. Faraday Soc. **48**, 749 (1952).

[3]D. C. Jilles and D. L. Atherton, J. Appl. Phys. **55**, 2115 (1984); A. A. Likhachev and Y. N. Koval, Scr. Metall. Mater. **27**, 1623 (1992).

[4]I. D. Mayergoyz, *Mathematical Models of Hysteresis*

(Springer-Verlag, Berlin, 1991); J. Ortín, J. Appl. Phys. **71**, 1454 (1992).

[5]J. P. Sethna, K. Dahmen, S. Kartha, J. A. Krumhansl, B. W. Roberts, and J. D. Shore, Phys. Rev. Lett. **70**, 3347 (1993).

[6]The existence of the RPM property is based on the Alan Middleton's no passing rule, formulated in the context of sliding charge-density waves in A. Middleton, Phys. Rev. Lett. **68**, 670 (1992); A. Middleton and D. S. Fisher, Phys. Rev. B **47**, 3530 (1993).

[7]E. Vives, J. Ortín, Ll. Mañosa, I. Ràfols, R. Pérez-Magrané, and A. Planes, Phys. Rev. Lett. **72**, 1694 (1994).

[8]P. J. Cote and L. V. Meisel, Phys. Rev. Lett. **91**, 1334 (1991); L. V. Meisel and P. J. Cote, Phys. Rev. B **46**, 10 822 (1992).

[9]P. Bak, C. Tang, and K. Wiesenfeld, Phys. Rev. Lett. **59**, 381 (1987).

[10]S. F. Edwards and P. W. Anderson, J. Phys. F **5**, 965 (1975).

[11]For a general review on spin glasses, see K. Binder and A. P. Young, Rev. Mod. Phys. **58**, 801 (1986).

[12]D. Sherrington and S. Kirkpatrick, Phys. Rev. Lett. **35**, 1972 (1975).

[13]G. Toulouse, Commun. Phys. **2**, 115 (1977).

[14]I. Morgenstern and K. Binder, Phys. Rev. B **22**, 288 (1980), and references therein.

[15]E. Domany, J. Phys. C **12**, L119 (1979).

[16]N. K. Jaggi, J. Phys. C **13**, L177 (1980).

[17]S. Wolfram, Nature (London) **311**, 419 (1984).

[18]J. Ortín showed us a sequence of electron microscope photographs revealing the back transformation of a martensite domain in a Cu-Zn-Al, while the temperature was being decreased, in a private communication.

[19]A spin-glass model of the RBIM type has also been useful for describing the pretransitional effects in systems undergoing martensitic transformation. See S. Kartha, T. Castan, J. A. Krumhansl, and J. P. Sethna, Phys. Rev. Lett. **67**, 3630 (1991).

[20]D. Stauffer, *Introduction to Percolation Theory* (Taylor & Francis, London, 1985).

[21]L. P. Kadanoff, S. R. Nagel, L. Wu, and S.-M. Zhou, Phys. Rev. A **39**, 6524 (1989).

[22]K. L. Babcock and R. M. Westervelt, Phys. Rev. Lett. **64**, 2168 (1990).

[23]P. Bak and H. Flyvbjerg, Phys. Rev. A **45**, 2192 (1992).

[24]D. Sornette, J. Phys. I (France) **4**, 209 (1994).